

SUPPORTING INFORMATION

Hyaluronan-tyrosine-gold nanoparticle as an enzyme-free colorimetric probe for the detection of phosphorothiolate pesticides

Limin Yang^a, Xiaohui Zhang^a, Huiping Li^a, Lei Jiang^{*a}

^aState Key Laboratory of Heavy Oil Processing and Center for Bioengineering and Biotechnology, China University of Petroleum (East China), Qingdao, Shandong 266555, P. R. China

*Corresponding author: Lei Jiang; Telephone: +86-053286981568; E-mail: leijiang@upc.edu.cn

This supporting information includes:

1. FT-IR characterization of HA-Tyr (Page S-2)
2. Possible interfering effect of the reducing ability of HA (Page S-2)
3. Characterization of AuNP surface HA-Tyr chains (Page S-3)
4. Stability of the HA-Tyr-AuNP (Page S-4)
5. DLS analysis of the HA-Tyr-AuNP before and after treatment with phorate (Page S-4)
6. The pH effect on the detection of phorate (Page S-5)
7. Comparison of the determination of phorate (Page S-5)

1. FT-IR characterization of HA-Tyr

In the presence of EDC and NHS, the carboxyl groups of HA can react with amino groups of Tyr-oMe resulting in the formation of HA-Tyr through amide linkages. The amide bond formation was characterized with FT-IR spectroscopy. As shown in Fig. S-1, characteristic peaks of HA appeared at 1610 and 1405 cm^{-1} for the asymmetric COO^- stretching vibration and the symmetric COO^- stretching vibration, respectively.¹ In the IR spectrum of graft HA-Tyr, these carbonyl absorption bands of carboxylate sodium salt in HA become weak and the new characteristic amide I band appears at 1660 cm^{-1} .² In addition, transmittance bands from the Tyr hydroxyl group (1250 cm^{-1}) and Tyr ring vibration (1515 cm^{-1}) appear in the IR spectra of HA-Tyr and Tyr³. These results suggest the graft of Tyr on HA.

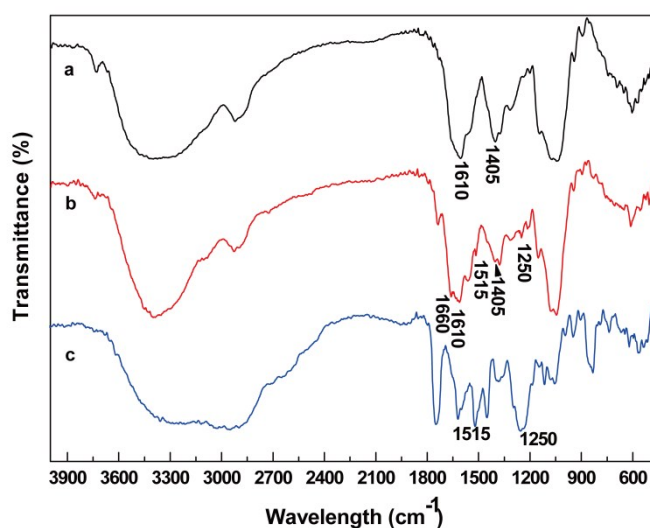


Fig. S-1 FT-IR spectra of HA (a), HA-Tyr (b), and Tyr-oMe (c).

2. Possible interfering effect of the reducing ability of HA

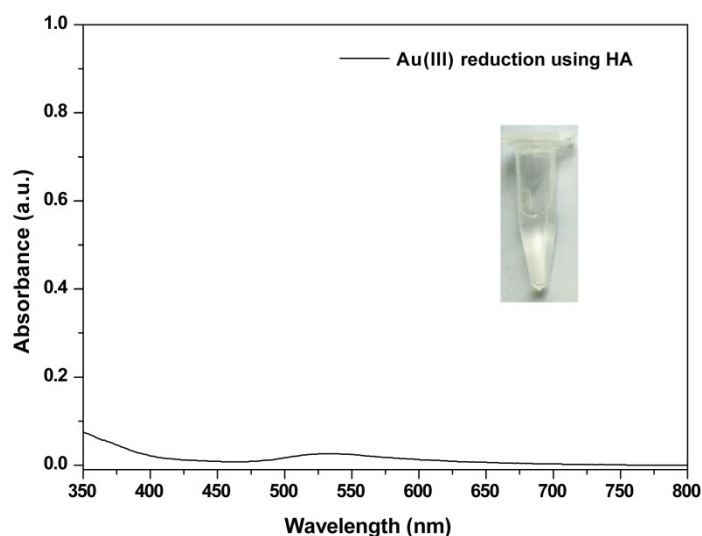


Fig. S-2 HA has very limited reducibility to reduce Au^{3+} ions at pH \sim 12.

3. Characterization of AuNP surface HA-Tyr chains

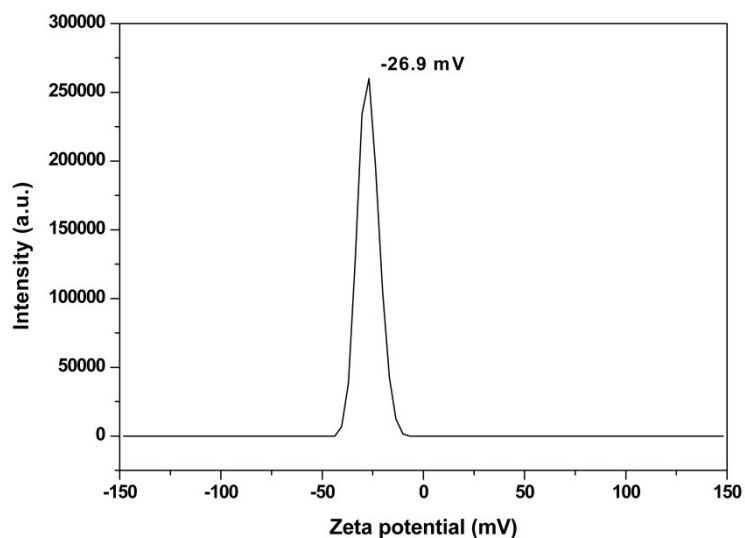


Fig. S-3 Zeta potential of HA-Tyr-AuNP.

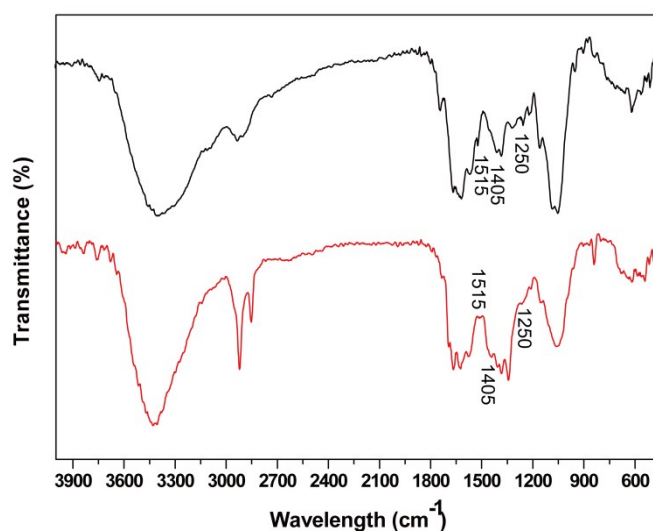


Fig. S-4 FT-IR spectra of free HA-Tyr (black line) and HA-Tyr-AuNP (red line).

Fig. S-4 shows the FT-IR spectra of HA-Tyr-AuNP after removing the excess unadsorbed HA-Tyr, which is compared with the pure HA-Tyr. The spectrum for HA-Tyr-AuNP conjugate shows two weak resonances at about 1515 and 1205 cm⁻¹, corresponding to the Tyr moieties of the HA-Tyr, and a 1405 cm⁻¹ band, corresponding to the carbonyl groups of the HA moieties. The presence of these characteristic peaks for the HA-Tyr implies their presence on the nanoparticle surface.

4. Stability of the HA-Tyr-AuNP

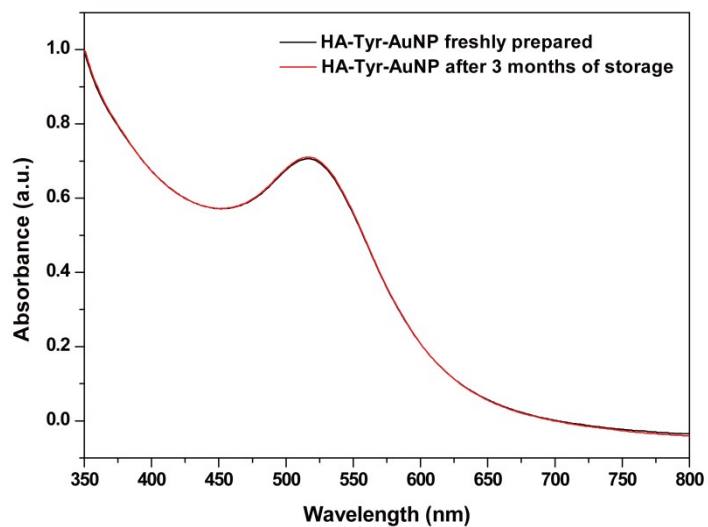


Fig. S-5 UV-vis spectra of the HA-Tyr-AuNP before and after 3 months of storage at room temperature.

5. DLS analysis of the HA-Tyr-AuNP before and after treatment with phosphate

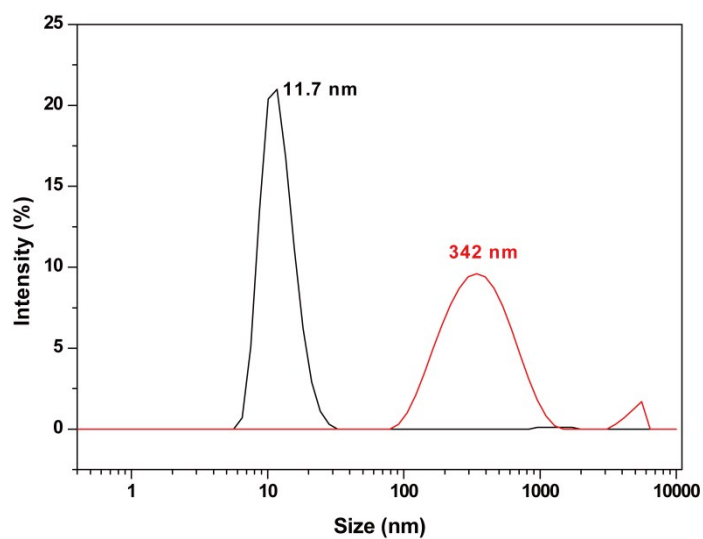


Fig. S-6 DLS measurements of HA-Tyr-AuNP solutions before (black line) and after (red line) adding phosphate.

6. The pH effect on the detection of phorate

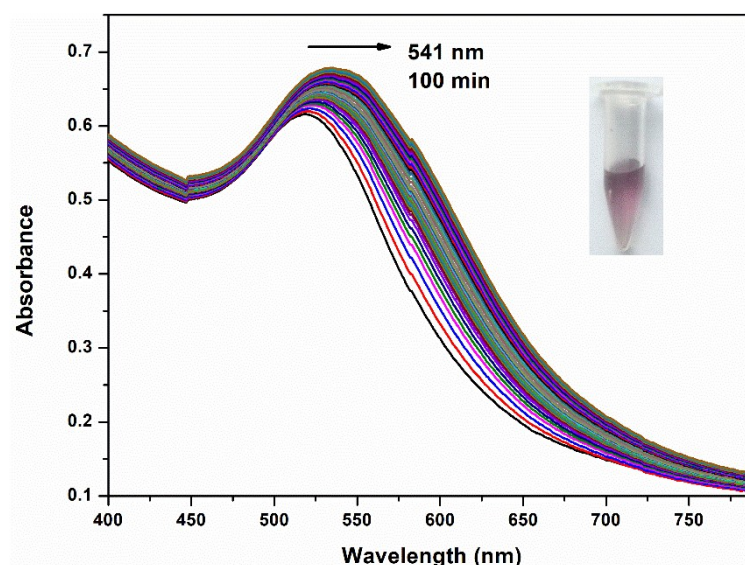


Fig. S-7 Time-dependent absorption of the HA-Tyr-AuNP after treating with $2 \mu\text{g mL}^{-1}$ phorate at pH 9. Inset: Photograph showing colorimetric response of detection system to phorate (after 2h). Note: To investigate the pH effect on the detection of phorate, the HA-Tyr-AuNP was first centrifuged from the colloidal solution at 10000 rpm for 10 min, then washed with water for three times, and re-dissolved in the media at different pHs. The media were 0.01 M phosphate-buffered solution (pH 9.0). The pH values were checked precisely by a FE-20 pH-meter (Mettler Toledo, China). The ionic strength (I) was carefully adjusted to 0.03 M by adding an appropriate amount of sodium chloride.

7. Comparison of the determination of phorate

Table S-1 Comparison of different phorate probing strategies

Methods	Linear range ($\mu\text{g mL}^{-1}$)	Detection limit ($\mu\text{g mL}^{-1}$)	Reference
Colorimetric method using rhodamine B-covered gold nanoparticle integrated with acetylcholinesterase	Not given	0.001	4
Capillary electrophoresis with laser-induced fluorescence using quantum dot-DNA aptamer conjugates	0.16-2.6	0.052	5
Fluorescence polarization assay with aptamer	Not given	0.0192	6
Surface enhanced Raman scattering method with Ag dendrites modified with aptamer and 6-mercaptophexanol	0-0.99	0.01	7
Surface enhanced Raman spectroscopic analysis with silver nanoparticles	Not given	0.05	8
Colorimetric method with hyaluronan-tyrosine-gold nanoparticles	0.005-1	0.005	This work

References

1. D. I. Ha, S. B. Lee, M. S. Chong, Y. M. Lee, S. Y. Kim and Y. H. Park, *Macromol. Res.*, 2006, **14**, 87-93.
2. K. Y. Cho, T. W. Chung, B. C. Kim, M. K. Kim, J. H. Lee, W. R. Wee and C. S. Cho, *Int. J. Pharm.*, 2003, **260**, 83-91.
3. F. DeLange, C. H. W. Klaassen, S. E. Wallace-Williams, P. H. M. Bovee-Geurts, X.-M. Liu, W. J. DeGrip and K. J. Rothschild, *J. Biol. Chem.*, 1998, **273**, 23735-23739.
4. D. Liu, W. Chen, J. Wei, X. Li, Z. Wang and X. Jiang, *Anal. Chem.*, 2012, **84**, 4185-4191.
5. T. Tang, J. Deng, M. Zhang, G. Shi and T. Zhou, *Talanta*, 2016, **146**, 55-61.
6. C. Zhang, L. Wang, Z. Tu, X. Sun, Q. He, Z. Lei, C. Xu, Y. Liu, X. Zhang, J. Yang, X. Liu and Y. Xu, *Biosens. Bioelectron.*, 2014, **55**, 216-219.
7. S. Pang, T. P. Labuza and L. He, *Analyst*, 2014, **139**, 1895-1901.
8. X. Li, S. Zhang, Z. Yu and T. Yang, *Appl. Spectrosc.*, 2014, **68**, 483-487.